Feedback Mechanisms Promote Cooperativity for Small Molecule Inhibitors of Epidermal and Insulin-Like Growth Factor Receptors

Elizabeth Buck,[1] Alexandra Eyzaguirre,[1] Maryland Rosenfeld-Franklin,[4] Stuart Thomson,[1]
Mark Mulvihill,[3] Sharon Barr,[1] Eric Brown,[4] Mathew O'Connor,[2] Yan Yao,[2]
Jonathan Pachter,[2] Mark Miglarese,[1] David Epstein,[1] Kenneth K. Iwata,[1]
John D. Haley,[2] Neil W. Gibson,[1] and Qun-Sheng Ji[2]

[1]Translational Research, [2]Cancer Biology, and [3]Cancer Chemistry, OSI Pharmaceuticals, Farmingdale, New York and
[4]In Vivo Pharmacology, OSI Pharmaceuticals, Boulder, Colorado

Abstract

Epidermal growth factor receptor (EGFR) and insulin-like growth factor-I receptor (IGF-IR) can cooperate to regulate tumor growth and survival, and synergistic growth inhibition has been reported for combined blockade of EGFR and IGF-IR. However, in preclinical models, only a subset of tumors exhibit high sensitivity to this combination, highlighting the potential need for patient selection to optimize clinical efficacy. Herein, we have characterized the molecular basis for cooperative growth inhibition upon dual EGFR and IGF-IR blockade and provide biomarkers that seem to differentiate response. We find for epithelial, but not for mesenchymal-like, tumor cells that Akt is controlled cooperatively by EGFR and IGF-IR. This correlates with synergistic apoptosis and growth inhibition *in vitro* and growth regression *in vivo* upon combined blockade of both receptors. We identified two molecular aspects contributing to synergy: (*a*) inhibition of EGFR or IGF-IR individually promotes activation of the reciprocal receptor; (*b*) inhibition of EGFR-directed mitogen-activated protein kinase (MAPK) shifts regulation of Akt from EGFR toward IGF-IR. Targeting the MAPK pathway through downstream MAPK/extracellular signal-regulated kinase kinase (MEK) antagonism similarly promoted IGF-driven pAkt and synergism with IGF-IR inhibition. Mechanistically, we find that inhibition of the MAPK pathway circumvents a negative feedback loop imposed on the IGF-IR–insulin receptor substrate 1 (IRS-1) signaling complex, a molecular scenario that parallels the negative feedback loop between mTOR-p70S6K and IRS-1 that mediates rapamycin-directed IGF-IR signaling. Collectively, these data show that resistance to inhibition of MEK, mTOR, and EGFR is associated with enhanced IGF-IR–directed Akt signaling, where all affect feedback loops converging at the level of IRS-1. [Cancer Res 2008;68(20):8322–32]

Introduction

The receptor tyrosine kinases (RTK) for epidermal growth factor (EGF) and insulin-like growth factor (IGF) contribute to tumorigenesis for a multitude of tumor types (1–4). Tumors can exhibit redundancy surrounding these RTKs that contributes to *de novo* resistance to a single RTK inhibitor, and crosstalk between RTKs can confer acquired resistance, whereby inhibition of one RTK is compensated by enhanced activity through the reciprocal RTK (5–14). These observations suggest that a combinatorial regimen targeting both EGF receptor (EGFR) and insulin-like growth factor-I receptor (IGF-IR) may yield greater anticancer activity.

Although the combination of EGFR and IGF-IR inhibitors has shown synergistic growth inhibition in preclinical models, the molecular mechanism for the cross-talk between EGFR and IGF-IR that mediates cooperativity has not yet been thoroughly investigated. Furthermore, the identification of molecular markers that could be used to refine patient subgroups most likely to receive maximal benefit from this specific combination therapy has not yet been described. We have recently reported the novel small molecule IGF-IR kinase inhibitor PQIP (15). Herein, we show that PQIP exhibits broad efficacy against a range of tumor types. Similar to observations made for erlotinib, sensitivity to IGF-IR inhibition seems to be greater in epithelial tumor cells compared with tumor cells that have undergone an epithelial-mesenchymal transition (EMT). PQIP synergized with erlotinib to inhibit cell growth and survival, and cooperativity was more extensive in epithelial than mesenchymal tumor cells. For epithelial tumor xenografts, the combination of erlotinib and PQIP promoted growth regressions during treatment and enhanced the durable cure rate.

We explored the molecular mechanism underlying the observed synergism for epithelial tumors. Inhibition of IGF-IR results in induced EGFR activity, highlighting reciprocity as one aspect contributing to cooperativity. Akt activity seems to be regulated through a combination of EGF and IGF signaling, and only dual targeting of both RTKs achieved complete and sustained Akt inhibition. Mechanistically, we find that inhibition of EGFR-directed mitogen-activated protein kinase (MAPK) pathway activity conveys enhanced coupling of IGF-IR to the phosphatidylinositol 3-kinase (PI3K)-PDK1-Akt pathway. Specifically, we show that ability of erlotinib to block activity within the MAPK pathway leads to inhibition of serine phosphorylation of insulin receptor substrate 1 (IRS-1), and this is associated with more effective signal flow from IGF-IR to Akt. Inhibition of the MAPK pathway using a specific inhibitor of MAPK/extracellular signal-regulated kinase kinase (MEK) also conferred enhanced IGF-driven Akt activity and sensitized tumor cells to PQIP. These results provide mechanistic understanding for the combined targeting of IGF-IR and EGFR and highlight the potential clinical utility of this combination.

Materials and Methods

PQIP. PQIP (*cis*-3-[3-(4-methyl-piperazin-l-yl)-cyclobutyl]1-(2-phenyl-quinolin-7-yl)-imidazo[1,5]pyrazin-8-ylamine) was synthesized, as previously described (15).

Cell lines. Cells were cultured in media, as prescribed by the American Type Culture Collection (ATCC) containing 10% FCS. With the exception of GEO (obtained from RPCI), all tumor cells were obtained from ATCC. Cell lines were designated as epithelial or mesenchymal, as described in Supplementary Materials and Methods.

Cell proliferation. Proliferation was determined using Cell Titer Glo (Promega), and apoptosis was determined by Caspase Glo (Promega), as previously described (16).

Analysis of cooperativity. The Bliss additivism model was used to analyze the cooperativity of drug interactions. This model and rationale for its use has been previously described (16).

Protein lysates and Western blotting. Lysates were prepared, as previously described (16). Antibodies (Cell Signaling) included EGFR, phosphorylated EGFR (Y1068), phosphorylated p42/p44, phosphorylated Akt (473), phosphorylated Akt (308), Akt, phosphorylated S6 (235/236), and S6. Where indicated, 10 ng/mL EGF or 40 ng/mL IGF were added for 5 min before lysis.

RTK proteome array. Proteome profiler arrays (R&D Systems) were processed according to manufacturer's protocol. RTKs included on the array are listed in Supplementary Materials and Methods.

IGF-IR ELISA. Cell lysates were transferred into 96-well plates precoated with IGF-IR capture antibody (Santa Cruz) and incubated overnight. Target protein was probed with an anti–pY-HRP–conjugated antibody (PY20; Zymed) followed by chemiluminescence detection (Pierce).

Quantitative PCR. cDNA was prepared, as previously described (17). Gene expression assays for IGF-I/ IGF-II (Applied Biosystems) were used to quantitate relative gene expression using 100 ng cDNA on an ABI 7300 system. Values were compared with amplification of glyceraldehyde-3-phosphate dehydrogenase (GAPDH).

Knockdown of IGF-IR and EGFR. IGF-IR and EGFR small interfering RNA (siRNA) were SmartPools (Dharmacon, NM_000875 and NM_201283). Nonspecific siRNA was from Qiagen. Cells were transfected using Lipofectamine 2000 (Invitrogen; ref. 16).

***In vivo* antitumor efficacy studies.** Female athymic nude *nu/nu* CD-1 mice (6–8 wk, 22–29 g; Charles River Laboratories) were maintained as previously described. Dosing of animals is described in Supplementary Materials and Methods.

Results

Multiple tumor types respond to IGF-IR inhibition by PQIP. Sensitivity to PQIP was determined for a panel of 27 tumor cell lines (Fig. 1*A*). Cells treated with 3 μmol/L PQIP (structure; Supplementary Fig. S1) exhibited a range of sensitivities (2–72% maximal growth inhibition), and the median growth inhibition, in response to 3 μmol/L PQIP, for the panel was 37% (Fig. 1*A*). PQIP (3 μmol/L) was selected as a dose to evaluate maximal growth inhibition; however, effects of varying concentrations of PQIP on proliferation was determined for all cell lines, and representative data is shown in Supplementary Fig. S1, demonstrating that growth inhibition by PQIP is dose-dependent. Selected tumor cell lines included in this panel harbor known activating mutations in PI3K (indicated by *; Fig. 1*A*), suggesting that their proliferation might be IGF-IR–independent. However, we find that PI3K mutations are not uniformly predictive of insensitivity to IGF-IR antagonism.

We have reported that epithelial tumor cells are more sensitive to EGFR inhibition than tumor cells that have undergone an EMT-like transition (17, 18), and recent reports have provided additional evidence that proteins related to EMT are predictive of sensitivity to EGFR inhibition for a variety of tumor types, including lung,

pancreas, colon, and bladder (17, 19, 20). Moreover, EMT biomarkers seem to be predictive of erlotinib response clinically (21). Herein, we find that EMT status also imparts differential sensitivity to IGF-IR inhibition, wherein epithelial tumor cells are substantially more sensitive than those that have undergone EMT. Seventy percent of epithelial tumor cells achieved growth inhibition greater than the median growth inhibition of the panel, and inhibition of >50% was not observed for any mesenchymal cell line. These data suggest that EMT markers could be useful to identify patients most likely to respond to IGF-IR inhibition.

Although all tumor cells evaluated expressed IGF-IR, expression level did not correlate with sensitivity (data not shown); however, sensitive tumor cells presented higher phosphorylated IGF-IR than insensitive tumor cells and epithelial tumor cells showed higher phosphorylated IGF-IR than mesenchymal tumor cells (Fig. 1*A* and Supplementary Fig. S2). These data support the enhanced dependence on IGF-IR for epithelial, compared with mesenchymal, tumors. Tumor cells expressed varying levels of IGF-I/IGF-II (Supplementary Fig. S2); however, autocrine expression did not uniformly correlate with sensitivity to IGF-IR inhibition. Sensitivity measurements were conducted in the presence of 10% FCS, where exogenous IGF could also drive IGF-IR signaling. Previous reports have indicated that although the growth of selected tumors can be driven by autocrine IGF signals, the growth of others is directed by IGF expressed by tumor-associated stromal cells in a juxtacrine manner (22, 23), suggesting that autocrine signals may not be required for IGF-IR dependence.

The IGF-IR inhibitor PQIP synergizes with the EGFR inhibitor erlotinib. We sought to determine the effects of combining the EGFR inhibitor erlotinib with PQIP and if EMT status might confer differential effects. Sensitivity to the combination of 3 μmol/L PQIP with 10 μmol/L erlotinib was determined for a panel of 22 tumor cell lines of varying EMT states. The maximal growth inhibition achieved for the combination is compared with that theoretically expected for additivity (Bliss analysis; Fig. 1*B, red line*). The combination achieved a median growth inhibition of 71% (Fig. 1*B, dashed red line*) in response to the combination of 3 μmol/L PQIP and 10 μmol/L erlotinib, and growth inhibition greater than this was observed only in epithelial tumor cell lines, suggesting that EMT status is an important marker of response. Six of thirteen epithelial tumor cell lines exhibited maximal growth inhibition of >95%. Mesenchymal tumor cell lines exhibited a greater range of sensitivities to the combination (7–75% growth inhibition); however, the majority (10 of 13) of mesenchymal cell lines showed lower sensitivity than the epithelial tumor cells, and the combination was synergistic only in a small population of mesenchymal lines. The growth inhibitory effects for combining erlotinib with PQIP were dose-dependent (Supplementary Fig. S3). Synergistic growth inhibition was reflected by both maximal growth inhibition and potency. For BxPC3 pancreatic tumor cells, the combination achieved an increase in maximal growth inhibition (40–98%), accompanied by an 8-fold gain in potency for PQIP (800–100 nmol/L).

The specificity of PQIP toward IGF-IR has been previously described; however, to confirm that the capacity for PQIP to synergize with erlotinib was due to inhibition of IGF-IR specifically, and not to other potential off-target effects, we evaluated the combination of erlotinib with neutralizing antibodies targeting IGF-IR. We find that two antibodies, MAB391 and α-IR3, cooperate with erlotinib to inhibit overall cell growth (Supplementary Fig. S4).
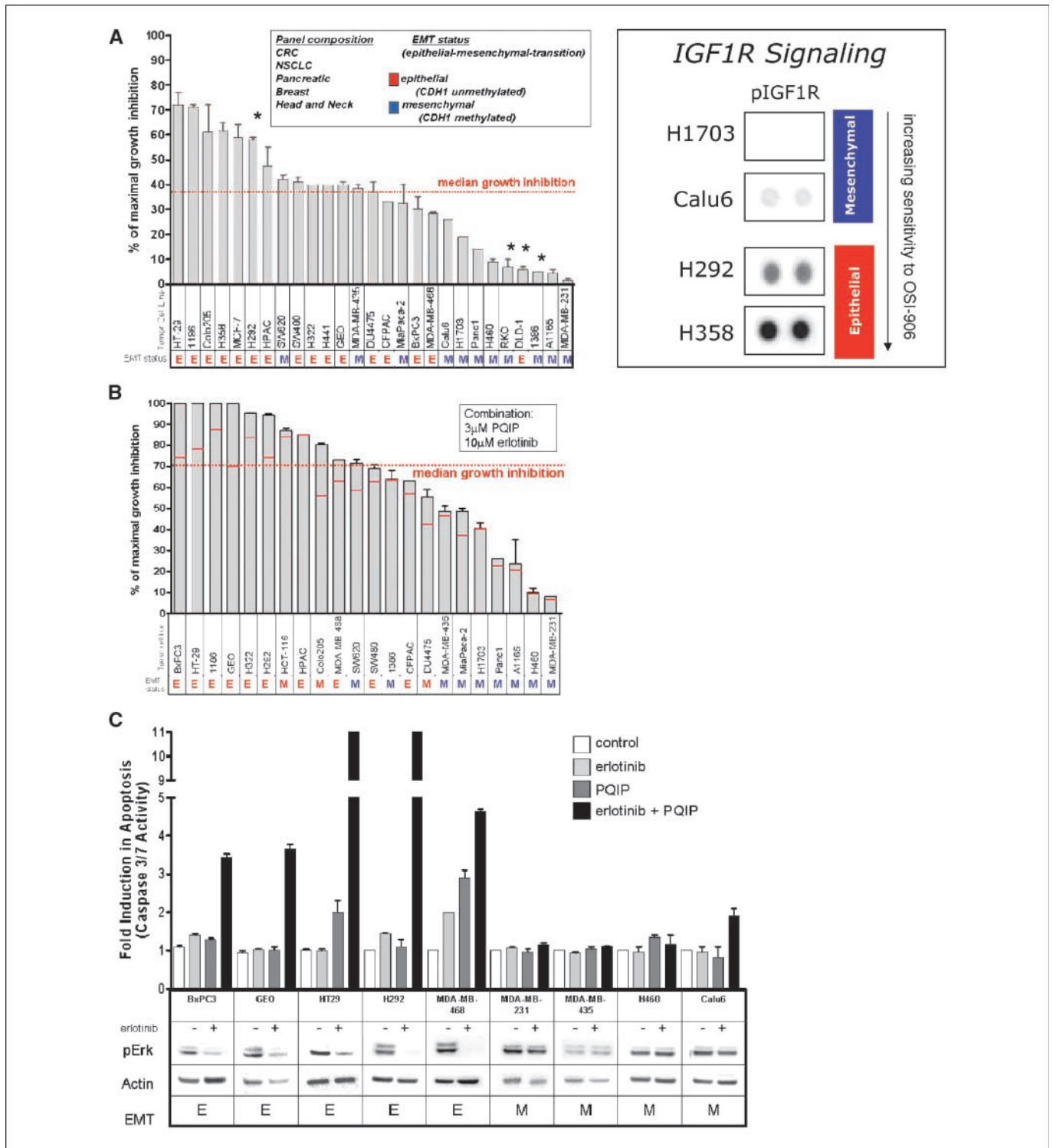
Figure 1. The combination of the IGF-IR inhibitor PQIP with erlotinib promotes cooperative inhibition of cell growth and survival. *A,* effect of 3 μmol/L PQIP on cell growth for a panel of 27 tumor cell lines (*left*). The EMT status for the cell lines is indicated, and those tumor cell lines which harbor a known activating mutation in PI3K are marked by a *. The average growth inhibition, calculated as the median of growth inhibition achieved within the panel, is indicated by a dotted line. The phosphorylation status of IGF-IR for two mesenchymal (H1703 and Calu6) and two epithelial (H358 and H292) cell lines (*right*). pIGF-IR was realized using the RTK proteome array as described in Materials and Methods. *B,* effect of 3 μmol/L PQIP in combination with 10 μmol/L erlotinib for a panel of tumor cells composed of both epithelial and mesenchymal lines. Erlotinib (10 μmol/L) was selected for screening, as this concentration has previously been shown to be biologically significant and clinically achievable (33–35). Data are expressed as percentage of maximal tumor growth inhibition and representative of three or more independent experiments. The theoretical expectation for additivity for the combination was calculated using the Bliss additivism model and is indicated by a red line. Tumor cells are characterized as either epithelial (*E*) or mesenchymal (*M*). The average growth inhibition, calculated as the median of growth inhibition for the panel achieved by the combination, is indicated by a dotted line. *C,* effect of 10 μmol/L erlotinib, 5 μmol/L PQIP, and the combination of 10 μmol/L erlotinib and 5 μmol/L PQIP on apoptosis, as measured by fold induction in caspase-3/caspase-7 activity measured 48 h after drug dosing. Data for five epithelial tumor cells (BxPC3, GEO, HT-29, NCI-H292, and MDA-MB-468) and four mesenchymal tumor cells (MDA-MB-231, MDA-MB-435, NCI-H460, and Calu6). The ability of erlotinib to affect Erk signaling is indicated.

Figure 1 *Continued. D,* effect of erlotinib (100 mg/kg, qd1-14; *open squares*), PQIP (75 mg/kg, qd1-14; *closed triangles*), or the combination of erlotinib and PQIP (100 mg/kg and 50 and 75 mg/kg, qd1-14; *open triangles and open diamonds*) on the growth of NCI-H292 xenograft tumors compared with vehicle-treated control mice (*closed diamonds*; *top*). Effect of erlotinib (100 mg/kg, qd1-10; *open squares*), PQIP (75 mg/kg, qd1-10; *closed triangles*), or the combination of erlotinib and PQIP (100 mg/kg and 75 mg/kg, qd1-10; *closed triangles*) on the growth of NCI-H441 xenograft tumors compared with vehicle-treated control mice (*closed diamonds*; *middle*). Effect of erlotinib (100 mg/kg, qd1-10; *open squares*), PQIP (75 mg/kg, qd1-10; *closed triangles*), or the combination of erlotinib and PQIP (100 mg/kg and 75 mg/kg, qd1-10, *closed triangles*) on the growth of NCI-H460 xenograft tumors compared with vehicle-treated control mice (*closed diamonds*; *bottom*). Erlotinib (100 mg/kg) was given orally by daily dosing with or without PQIP (25, 50, or 75 mg/kg). In comparison, a subset of mice received 75 mg/kg PQIP alone. Once daily, 75 mg/kg PQIP were selected for single-agent dosing. Previous studies had indicated that 75 mg/kg PQIP achieved plasma concentrations of ~ 5 μmol/L PQIP at 2 h after dosing, which was associated with inhibition of tumoral IGF-IR phosphorylation and which was sustained for 24 h (15). For evaluating the effects of combining PQIP with erlotinib on the growth of established xenograft tumors, 75, 50, and 25 mg/kg doses were selected, as *in vitro* studies have shown that erlotinib can improve the potency for PQIP, and therefore, lower doses may be sufficient to affect tumor growth.
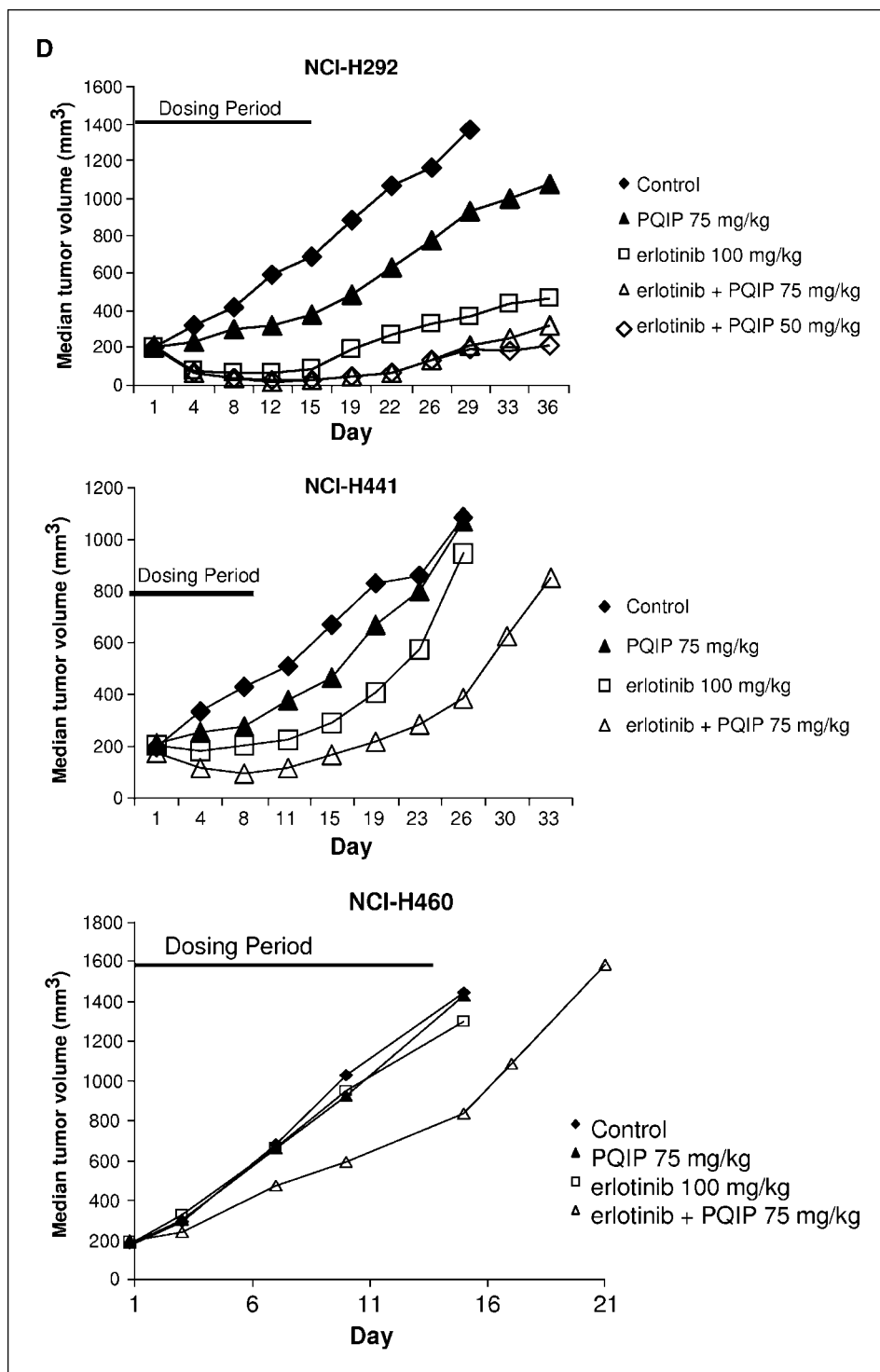
We sought to determine if the combination of PQIP and erlotinib could evoke inhibition of cell survival (Fig. 1*C*). For epithelial, but not mesenchymal, tumor cells, erlotinib achieved inhibition of downstream pErk signaling. Erlotinib alone achieved minimal apoptosis for evaluation, consistent with its predominant single-agent activity being cytostatic. PQIP achieved varying extents of apoptosis, and three epithelial tumor cell lines were among those that achieved a 2-fold to 5-fold induction in apoptosis. However, in combination, erlotinib synergized with PQIP to promote apoptosis in all epithelial tumor cell lines tested, whereas this effect was either absent or more modest for mesenchymal tumor cells. The synergistic apoptosis was dose-dependent and is shown for two representative epithelial models, NCI-H292 and BxPC3 (Supplementary Fig. S5*A, top* and *bottom*, respectively). Collectively, these data show how EMT markers might predict tumors most likely to respond to the combined blockade of IGF-IR and EGFR.

To further establish cooperativity between EGFR and IGF-IR, the effect of erlotinib, PQIP, or the combination (±IGF) was
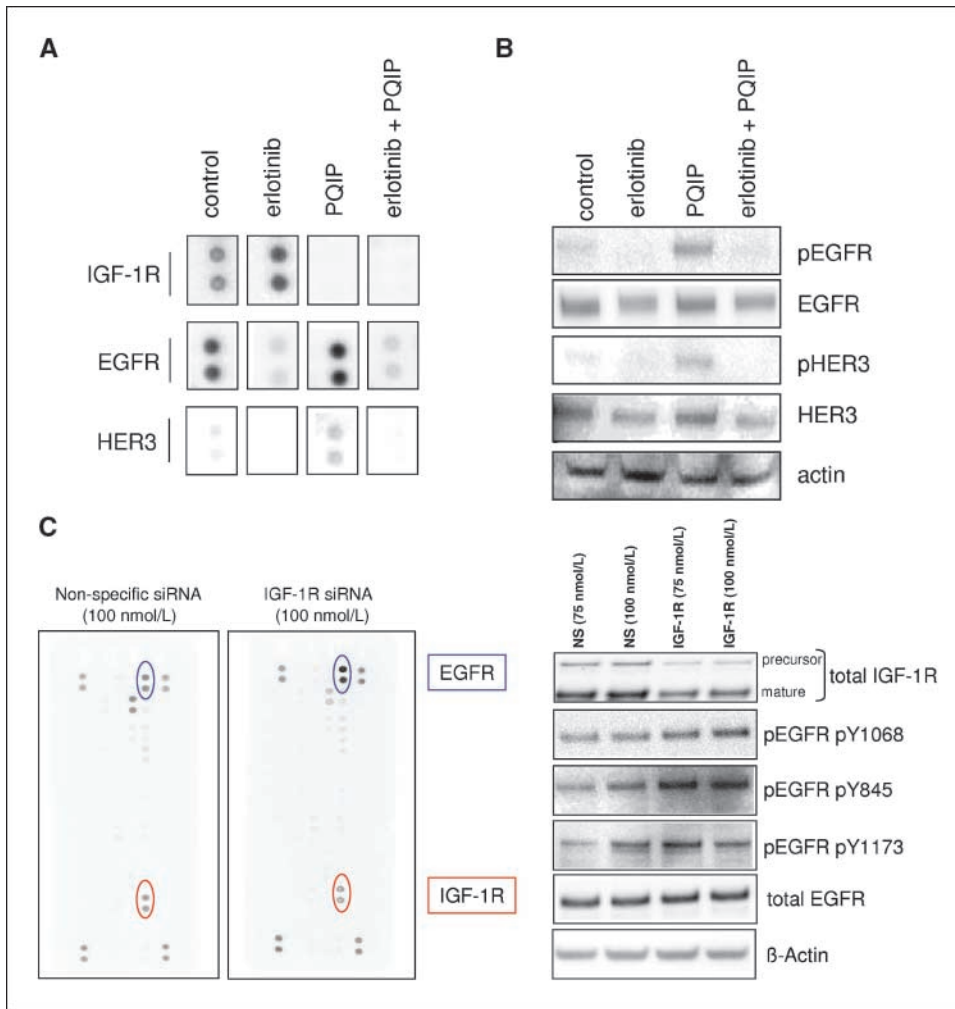
Figure 2. Inhibition of EGFR or IGF-IR individually results in up-regulation of activity in the alternate RTK. The effect of erlotinib (10 μmol/L), PQIP (5 μmol/L), or the combination of erlotinib (10 μmol/L) and PQIP (5 μmol/L) on the phosphorylation for a panel of 42 RTKs was determined for GEO cells using a proteome array. Effects on IR, IGF-IR, EGFR, and HER3 phosphorylation as measured by array (*A*) or effects on EGFR and HER3 phosphorylation as measured by Western blotting (*B*). Effect of siRNA toward IGF-IR (100 nmol/L) in BxPC3 tumor cells on the phosphorylation state for a panel of RTKs (*C, left*) realized by the capture array method. Effect of 75 or 100 nmol/L siRNA toward IGF-IR in BxPC3 tumor cells on the total receptor expression for IGF-IR and EGFR, and the specific EGFR tyrosine phosphorylation states pEGFR-Y1068, pEGFR-Y845, and pEGFR-Y1173 as realized by Western blotting (*C, right*). Results shown are typical of three or more experiments.

determined for NCI-H292 and NCI-H441 cells by measuring poly(ADP-ribose) polymerase or caspase-3 cleavage (Supplementary Fig. S5*B*). By this sensitive approach, erlotinib achieved measurable apoptosis for both cell lines; however, this was inhibited by exogenous IGF, indicating that IGF-IR signaling can circumvent EGFR inhibition to maintain cell survival. In the presence of IGF, enhanced apoptosis was detected in cells treated with the combination.

The combination of erlotinib and PQIP achieves tumor growth regression *in vivo*. The antitumor efficacy of PQIP and erlotinib was evaluated using mouse xenografts for two epithelial (NCI-H292 and NCI-H441) and one mesenchymal (NCI-H460) tumor (Fig. 1*D*). Consistent with *in vitro* observations, no significant effect on tumor growth for the mesenchymal model NCI-H460 was observed by either erlotinib or PQIP alone (Fig. 1*D*). When 75 mg/kg PQIP was coadministered with erlotinib, modest
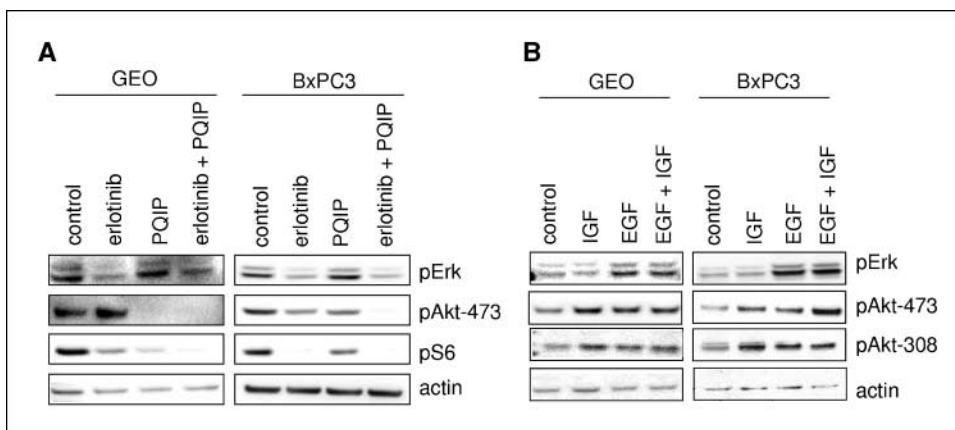

Figure 3. Erk activity is regulated by erlotinib alone, but Akt activity is regulated by both erlotinib and PQIP. *A,* effect of erlotinib (10 μmol/L), PQIP (5 μmol/L), or the combination on pErk, pAkt-473, and pS6 for GEO and BxPC3 cells. *B,* effect of IGF (10 ng/mL), EGF (10 ng/mL), or the combination of IGF and EGF on pErk, pAkt-473, and pAkt-308 for serum-starved BxPC3 and GEO cells.
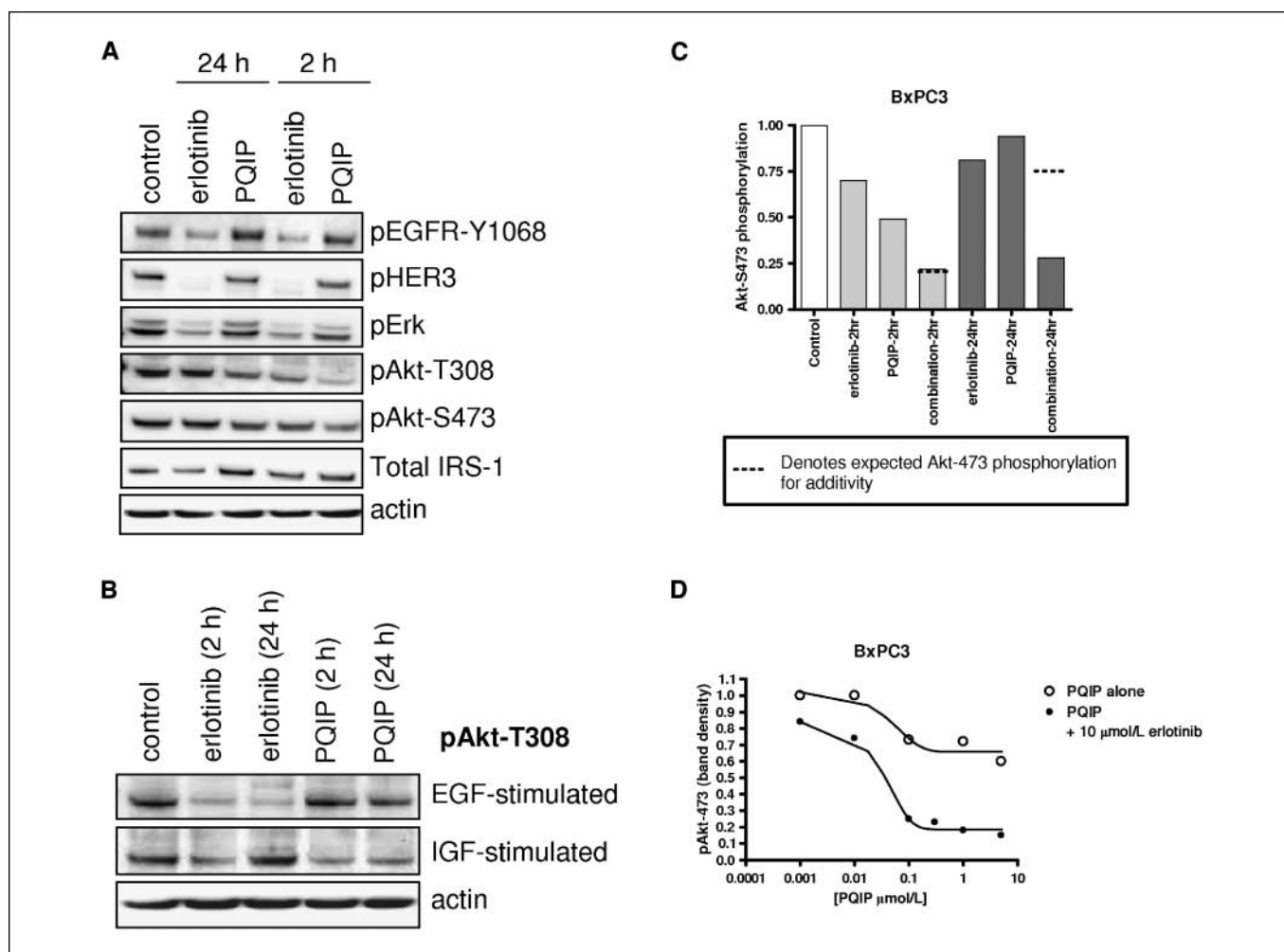
Figure 4. Akt activity is inhibited by erlotinib and PQIP additively 2 h after dosing but is inhibited cooperatively at 24 h postdosing. *A,* effect of 2-h or 24-h treatment of erlotinib (10 μmol/L) or PQIP (5 μmol/L) for BxPC3 cells on pEGFR, pHER3, pErk, pAkt-473, pAkt-308, pS6, and total IRS1. *B,* effect of 2-h and 24-h treatments with either erlotinib or PQIP on pAkt-308 for EGF-stimulated or IGF-stimulated BxPC3 cells. For control, cells were treated with either EGF or IGF, as indicated, in the absence of either erlotinib or PQIP. *C,* effect of 2-h or 24-h treatment of erlotinib, PQIP, or the combination on pAkt-473 levels for BxPC3 cells. The level of pAkt-473 was determined by Western blot band density for pAkt-473 normalized to GAPDH. The expected inhibition of pAkt for additivity is shown as a dotted line. *D,* effects of varying concentrations of PQIP, alone or in combination with 10 μmol/L erlotinib on pAkt-473 24 h postdosing. Results shown are typical of three or more experiments.

but statistically significant antitumor activity (51% TGI) was achieved (Fig. 1*D*; Supplementary Table S1). However, in this mesenchymal tumor model, the combination failed to achieve growth regression or meaningful growth delay. In contrast, we observed enhanced activity for the two epithelial models, NCI-H292 and NCI-H441. Erlotinib (10 mg/kg) alone resulted in 100% TGI that was accompanied by 71% maximum tumor regression. Once daily PQIP (75 mg/kg) alone resulted in ~59% TGI without evidence of regression (Fig. 1*D*). However, when PQIP was dosed at 50 or 75 mg/kg in combination with erlotinib, the antitumor efficacy achieved for the NCI-H292 xenografts was statistically significantly greater than that observed with erlotinib alone, as shown by an increase in maximum regression to >90% in each combination group. Additionally, when 50 mg/kg PQIP was dosed with erlotinib, a 37.5% durable cure rate (three of eight mice) was observed (Supplementary Table S1; Fig. 1*D*). In a similar manner, coadministration of PQIP with erlotinib exhibited more potent antitumor activity in NCI-H441 epithelial xenografts than either of

the inhibitors alone. For the group receiving 100 mg/kg erlotinib in combination with 75 mg/kg PQIP, ~48% maximum tumor regression was observed. In contrast, no evidence of tumor regression was found in mice dosed with either agent alone, and <5% regression was observed with erlotinib alone (Supplementary Table S1; Fig. 1*D*). For these three models, the highest dose combinations resulted in 22% to 25% body weight loss, suggesting this is the maximum tolerated dose in the mice. However, we do not feel that body weight loss is contributing to improved efficacy because no tumor regressions were seen in the NCI-H460 model although 22% body weight loss was observed. Hence, the growth modulation observed for these non–small cell lung cancer (NSCLC) cells *in vitro* correlated with their responsiveness to erlotinib and PQIP combination treatments *in vivo*, and collectively, these data suggest that epithelial tumors will maximally benefit from this combination.

IGF-IR inhibition augments EGFR signaling. We sought to explore whether resistance to IGF-IR inhibition was specific to

EGFR or if other RTKs could also compensate. We screened for changes in RTK phosphorylation using an antibody array for 42 RTKs against GEO tumor cells treated with erlotinib, PQIP, or the combination. Treatment with 5μmol/L PQIP resulted in inhibition of IGF-IR that was accompanied by an increase in the phosphorylation of EGFR and HER3 (Fig. 2*A*). We also observed a small but significant (~2-fold) increase in IGF-IR phosphorylation in cells treated with erlotinib. We found no detectable changes in the phosphorylation of any other RTK included in this panel (data not shown), indicating that pathways giving rise to resistance to IGF-IR inhibitors might be primarily driven by EGFR. By Western blotting, we confirmed a clear increase in EGFR and HER3 phosphorylation for GEO cells upon treatment with PQIP (Fig. 2*B*). EGFR transactivation of HER3 confers activation of the PI3K-Akt pathway in epithelial tumor cell lines, indicating that Akt signaling through EGFR specifically, and not other RTKs, might limit the sensitivity to IGF-IR antagonism (24). HER3, whose expression is repressed by transcription factors important for EMT, has been previously shown to be predominantly expressed in epithelial tumor cell lines, and we have found that erlotinib inhibits Akt primarily in epithelial tumor cells (24, 25). These data are consistent with our initial observations, herein, where synergistic growth inhibition and apoptosis by the EGFR and IGF-IR inhibitor combination occurs primarily in epithelial tumor cell lines, providing a mechanism underlying EMT status as a biomarker predictive of response to combined blockade of EGFR and IGF-IR.

We further investigated the capacity for inhibition of IGF-IR to confer increased EGFR activity by molecular approaches. Using siRNA toward IGF-IR, we obtained a partial knockdown of protein levels for BxPC3 epithelial tumor cells (Fig. 2*C, right*). Consistent with data obtained for PQIP, IGF-IR knockdown conferred increased phosphorylated EGFR (Fig. 2*C, left*). Antibodies toward specific phosphorylation sites of EGFR-Y1068/Y845/Y1173 revealed an increase in pEGFR by >2-fold upon knockdown of IGF-IR (Fig. 2*C, right*). These data confirm that inhibition of IGF-IR specifically, by PQIP, is responsible for the evoked increase in EGFR activity.

Erlotinib exibits a high degree of selectivity for EGFR, inhibiting EGFR with >200-fold (HER2) and >1000-fold (within a panel of 20 other kinases evaluated) selectivity over other kinases; therefore, erlotinib provides a very specific pharmacologic tool to evaluate changes in cellular signaling upon inhibition of EGFR. However, we sought to confirm, by other methods, the capacity of EGFR signaling to affect cellular dependence on IGF-IR. Using siRNA, we obtained a partial knockdown of EGFR protein levels (~40%), which was associated with a partial induction in IGF-IR phosphorylation of ~1.8-fold for BxPC3 cells (Supplementary Fig. S5*C, left*). To further confirm how changes in EGFR signaling affect sensitivity to inhibition of the IGF-IR pathway, we determined the effect of EGF treatment on the sensitivity to PQIP for H292 tumor cells. As inhibition of EGFR had increased signaling through IGF-IR and sensitivity to the IGF-IR antagonist PQIP, we find that increased signaling through EGFR, upon stimulation with exogenous ligand, blocks cellular dependence on IGF-IR, as indicated by the decreased sensitivity to the IGF-IR inhibitor PQIP (Supplementary Fig. S5*C, right*). This was reflected by both a 2-fold decrease in potency and reduced maximal growth inhibition (65–32%) for the IGF-IR inhibitor. Collectively, these data illustrate the cooperativity between IGF-IR and EGFR to affect cellular growth.

Akt is regulated cooperatively by IGF and EGF for epithelial tumor cells. For the epithelial tumor cell lines GEO and BxPC3,
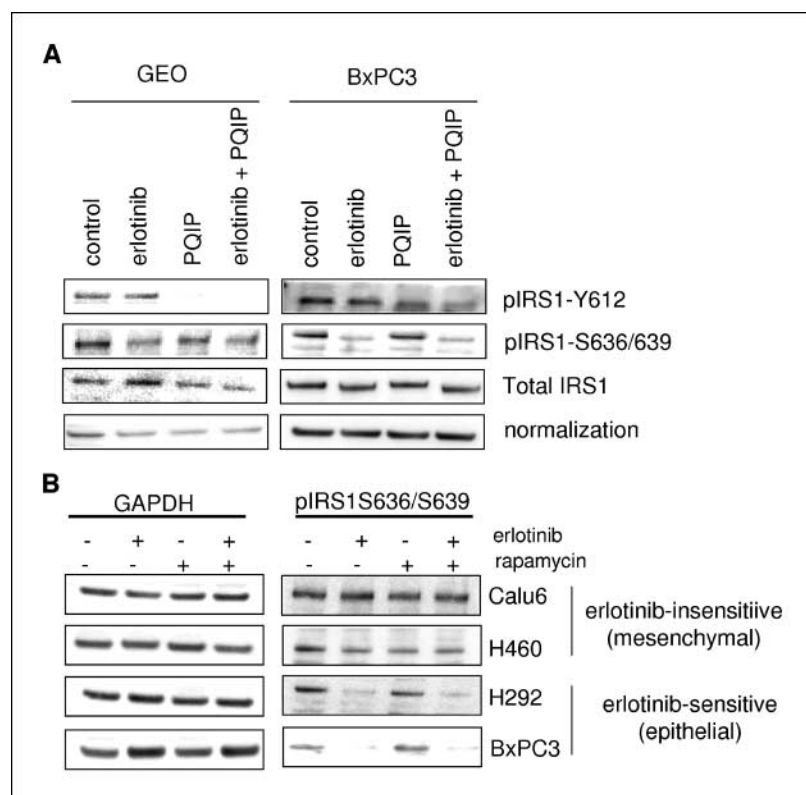

Figure 5. Inhibition of pIRS-1-S636-639 by erlotinib occurs only in epithelial tumor cells where erlotinib inhibits pErk. *A,* effects of erlotinib (10 μmol/L), PQIP (3 μmol/L), or the combination of both erlotinib and PQIP on the expression of total IRS-1 and the phosphorylation of IRS-1 (S636/639) and IRS-1 (Y612) for GEO and BxPC3 cells. *B,* effect of 10 μmol/L erlotinib, 10 nmol/L rapamycin, or the combination on the phosphorylation of IRS-1-(S636-639) and for two mesenchymal tumor cells (NCI-H460 and Calu6) and two epithelial tumor cells (NCI-H292 and BxPC3).
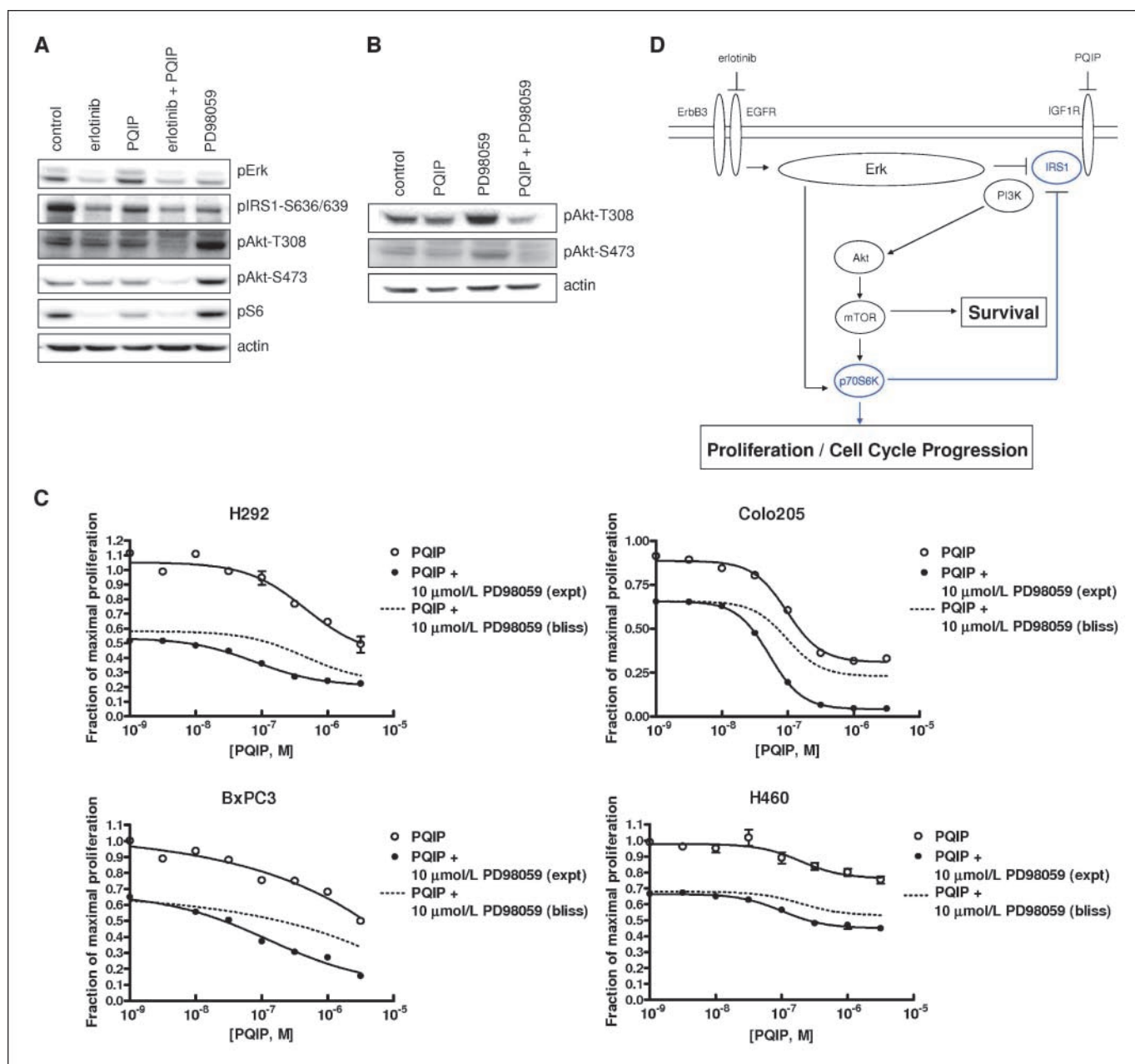
Figure 6. Inhibition of the MAPK pathway promotes Akt phosphorylation and cell survival, and this is blocked by PQIP. *A*, effect of 24-h treatment of BxPC3 cells with erlotinib, PQIP, the combination of erlotinib (10 μmol/L) and PQIP (5 μmol/L), or PD98059 (3 μmol/L) on the phosphorylation of Erk, IRS-1 (S636-639), IRS-1 (Y896), Akt (308), Akt (473), and S6. *B*, effect of PD98059, alone or in combination with PQIP, on the phosphorylation of Akt for both the T308 and S473 sites for BxPC3 cells. *C*, effect of varying concentrations of PQIP, alone, or in combination with PD98059, on the growth of BxPC3, NCI-H292, NCI-NCI-H460, and Colo205 cells. *D*, cartoon depicting the feedback loops where inhibition of EGFR activity confers enhanced activity through the IGF-IR-IRS-1-PI3K-Akt pathway.

erlotinib, but not PQIP, affected Erk phosphorylation, and under serum-starved conditions, only EGF activated Erk (Fig. 3A and B). However, activity within the Akt-mTOR-S6 pathway seemed to be regulated jointly by EGFR and IGF-IR. When BxPC3 cells were treated with erlotinib or PQIP for 2 hours, pAkt-S473 levels were reduced to ~50%, and the combination of erlotinib and PQIP achieved an additive decrease in pAkt-S473. Under serum-starved conditions, both IGF and EGF could stimulate pAkt-S473/T308 (Fig. 3B). For GEO cells, although we observed inhibition of pAkt-S473 only by PQIP, we were able to detect both IGF-driven and EGF-driven pAkt-S473/T308 under serum-free conditions.

We selected BxPC3 cells as our model to explore the mechanism, whereby the EGFR and IGF-IR pathways couple to regulate Akt and promote survival. Under 10% FCS conditions, erlotinib inhibited pAkt-S473/T308 after 2 hours of treatment; however, significant inhibition of pAkt was not sustained after 24 hours of treatment, despite the ability of erlotinib to inhibit EGFR-HER3 signaling, equivalently at both time points (Fig. 4A). We observed a similar trend for IGF-IR inhibition, where PQIP was substantially more effective in inhibiting pAkt-S473/T308 after 2 hours of treatment than 24 hours (Fig. 4A). At 24 hours PQIP treatment, we also observe an increase in pEGFR for BxPC3

cells, consistent with results obtained for GEO cells. To test whether erlotinib acted to promote IGF-driven Akt, by 24 hours after treatment, we treated BxPC3 cells with either erlotinib or PQIP for 2 or 24 hours followed by 5-minute stimulation with EGF or IGF (Fig. 4*B*). Erlotinib-inhibited EGF-stimulated pAkt-T308 equally well at both time points. However, for IGF-treated cells, we find that, whereas erlotinib inhibited pAkt in cells treated for 2 hours, erlotinib had no effect on pAkt in 24-hour treated cells although erlotinib was still bioactive at 24 hours after dosing, as shown by its ability to still inhibit EGF-stimulated Akt and its ability to achieve equivalent inhibition of EGFR and HER3 at both 2 and 24 hours after dosing (Fig. 4*A*). These data indicate the enhanced potential for IGF to drive pAkt after prolonged erlotinib treatment. Furthermore, although the single-agent inhibitors of EGFR and IGF-IR are both less efficacious after 24 hours of treatment, the combination is equally efficacious (Fig. 4*C* and Supplementary Fig. S5). The combination achieved additive Akt inhibition at 2 hours after dosing but synergistic inhibition of Atk at 24 hours after dosing. Herein, synergy was defined as inhibition of Akt greater than that calculated using the BLISS model. The ability of erlotinib to inhibit Akt phosphorylation synergistically with PQIP is dose-dependent (Fig. 4*D*). The combination of erlotinib and PQIP maximally achieved 84% inhibition of Akt; >50% inhibition theoretically expected based upon the BLISS model. Collectively, these data indicate how inhibition of EGFR by erlotinib is accompanied by enhanced IGF-IR signaling, which acts to sustain activation of the Akt pathway.

Erlotinib enhances IGF-IR signaling by promoting signal flow through the IGF-IR/IRS-1/Akt axis. We sought to explore the mechanism whereby erlotinib could enhance IGF-driven Akt activity. IGF-IR relies on a scaffold, IRS-1 to relay signals to downstream effectors. The phosphorylation of IRS-1 on Y-sites by IGF-IR provides docking sites for the SH2 domain of p85-PI3K (26–28). Scaffold functions for IRS-1 are elegantly regulated through both tyrosine and serine phosphorylation. Whereas Y-phosphorylation promotes the ability of IGF-IR to couple to Akt, S-phosphorylation inhibits IRS-1 functions. S-phosphorylation inhibits IRS-1 activity through several proposed mechanisms including (*a*) promoting ubiquitination and down-regulation, (*b*) sterically blocking interactions with IGF-IR and/or docking effectors, (*c*) altering the subcellular localization (27). *S*-phosphorylation of IRS-1 can be achieved by multiple feedback loops within the cell. p70S6 kinase, which lies downstream of the Akt-mTOR cascade, has been reported to phosphorylate IRS-1 and promote its inactivation. Inhibition of signaling downstream of mTOR has been shown to promote IGF-driven Akt activity. The mTOR inhibitor rapamcyin conveys an increase in IGF-dependent Akt activity for selected tumor cells, and synergistic growth inhibition for the combination of rapamycin with an IGF-IR inhibitor has been recently reported (29). Indeed, we have also observed synergistic growth inhibition for the combination of PQIP with Rapamycin (data not shown).

We wondered whether erlotinib might also promote IGF-driven Akt activity by affecting the phosphorylation state of IRS-1. We measured the ability of the EGFR or IGF-IR inhibitors to affect IRS-1 phosphorylation at selected pY and pS sites for BxPC3 and GEO cells. pY612-IRS-1 is inhibited by PQIP (Fig. 5*A*) and IGF can drive pY612-IRS-1 in serum-starved cells (data not shown). Previous reports have indicated that IRS-1-Y612 serves as a docking node for p85-PI3K. Whereas PQIP had no effect on

pIRS-1-S636/639, we find that erlotinib could inhibit pIRS-1-S636/639. S636/639 specifically has been reported to block IRS-1 function. Therefore, these data suggest that erlotinib might potentiate IGF-IR signaling by enhancing the ability of IGF-IR to couple to IRS-1.

Erk and p70S6K have been previously reported to phosphorylate IRS-1, and the activities for both can be inhibited by erlotinib. We sought to determine if inhibition of Erk, p70S6K, or both were involved in mediating the ability of erlotinib to affect IRS-1 phosphorylation. We measured the ability of erlotinib or rapamycin to affect pIRS-1-S636/639 for mesenchymal (NCI-H460 and Calu6) and epithelial (NCI-H292 and BxPC3) tumor cell lines. Herein, we find that erlotinib can inhibit pIRS1-S636-639 only in the epithelial cell lines (Fig. 5*B*) consistent with our observations of enhanced synergistic effects for its combination with PQIP in epithelial, compared with mesenchymal, tumor cell lines.

EGFR-activated Erk could relay signals through p70S6K, thereby activating p70S6K by a rapamycin-insensitive mechanism, to enhance pIRS-1-S636-639. The ability of EGFR-activated p70S6K to promote phosphorylation of IRS1-S636-639 and, in turn, inhibit IGF-IR-IRS1 signaling would parallel a similar negative regulatory feedback loop that has been proposed to underlie the synergism observed for the combination of an IGF-IR inhibitor and rapamycin. As an alternate mechanism, EGFR-activated Erk could directly phosphorylate pIRS1-S636-639 (Fig. 6*D*). The ability of MAPK to phosphorylate IRS-1 *in vitro* has been reported (30). *In silico*, we evaluated the propensity for the IRS1-S636-639 sites to be phosphorylated by a panel of kinases using the Scansite program (31). Scansite uses a database obtained from profiling the consensus phosphorylation patterns for a wide number of kinases and, thus, allows prediction of kinase-substrate pairs. Among the evaluated kinases, the sequence surrounding the IRS1-636-639 sites (PM*S*P) ranks highest as a substrate for Erk and contains the PX*S*P Erk-consensus motif. We find that, although erlotinib was effective at inhibiting pIRS1-S636-639, rapamycin had no measurable effect in either the NCI-H292 or BxPC3 models. Rapamycin is effective at inhibiting signals downstream of mTOR, including p70S6K and S6, but does not affect activity for the MAPK pathway. Therefore, we speculate that ability of erlotinib to block MAPK pathway activity was likely associated with the inhibition of IRS-1 serine phosphorylation. To validate this hypothesis, we treated BxPC3 cells with a specific inhibitor of MEK, PD98059, and monitored the phosphorylation status for pS-IRS-1 and pAkt. We find that inhibition of downstream Erk by PD98059 was accompanied by inhibition of pS-IRS-1, thus relieving a potential inhibitory loop imposed on IGF-IR-IRS-1-PI3K signaling (Fig. 6*A*). This generated an increase in Akt phosphorylation (T308 and S473). The increase in pAkt, evoked by inhibition of the MAPK pathway, could be blocked by PQIP (Fig. 6*B*), indicating that this Akt activation was IGF-driven. These data suggest that the gain in IGF-IR–directed Akt activity upon EGFR inhibition is likely due, at least in part, to the release of a negative regulatory feedback loop involving MEK-Erk-IRS-1 that would normally attenuate IGF-IR.

To confirm that inhibition of the EGFR-MAPK pathway mediated enhanced sensitivity to IGF-IR antagonism, we evaluated the combination of PQIP and PD98059. This combination achieved synergistic growth inhibition in all models evaluated (BxPC3, NCI-H292, Colo205, and NCI-H460; Fig. 6*C*). Collectively, these

results show how the ability of erlotinib to inhibit activity within the MAPK pathway contributes to an increase in IGF-driven Akt activity.

Discussion

Both IGF-IR and EGFR play key roles in the growth and progression of solid tumors, and interactions between IGF-IR and EGFR have been previously shown (8, 10, 14). EGFR inhibitors are clinically approved for NSCLC, pancreatic cancer, SCCHN, and CRC, and both antibody and small molecule inhibitors of IGF-IR are currently in clinical development. Data suggests that the IGF-IR pathway may be one of the key mechanisms for *de novo* and acquired resistance to EGFR inhibition, and blockade of both IGF-IR and EGFR functions may be required for optimal efficacy. The translation of these preclinical observations to clinical efficacy may require enrichment strategies based on biomarkers that identify patients most likely to respond to this specific combination of agents. Despite impressive preclinical data for the combination of EGFR and IGF-IR inhibitors, the underlying molecular mechanism that drives the success for this specific combination of RTK inhibitors for selected tumor models, but not others, has not yet been thoroughly described.

Herein, we describe the signal transduction mechanisms that underlie cooperative EGFR and IGF-IR signaling. We used the low molecular weight inhibitors of EGFR (erlotinib) and IGF-IR (PQIP) as tools. Blockade of IGF-IR individually achieved growth inhibition for a range of tumor types. Overall, epithelial tumor cells achieved enhanced growth inhibition compared with those that had undergone EMT. Seven of 28 tumor cells achieved maximal growth inhibition >50% upon IGF-IR blockade, and these were all epithelial. Dual blockade of EGFR and IGF-IR promoted synergistic growth inhibition. Although treatment with single-agent inhibitors of these RTKs was predominately cytostatic, treatment with the combination of EGFR and IGF-IR inhibitors resulted in the induction of apoptosis, and these effects were most prominent for epithelial, compared with mesenchymal, tumor cells. Furthermore, statistically significant growth regression *in vivo* was achieved for the combination in epithelial tumors, and in the NCI-H292 NSCLC model, about one third of animals had durable cures.

Observations presented herein suggest that the expression of EMT markers can be used to differentiate the sensitivities of tumor cell lines to IGF-IR inhibitors, alone or in combination with an EGFR inhibitor. For many of the tumor types addressed in this study (NSCLC, pancreatic, etc.) the relative proportion of epithelial to mesenchymal tumor cells within a given tumor is related to disease stage, where stage 1 tumors are largely composed of epithelial tumor cells and there is rise in the proportion of mesenchymal tumor cells with increasing disease stage. Therefore, the biomarker signature for IGF-IR inhibitor sensitivity, alone or in combination with an EGFR inhibitor, seems to be confined to early stage disease, a finding that is supported by recent histopathologic data where IGF-IR overexpression was shown to be a poor prognostic indicator (HR > 3) for stage 1 but not for other stage (HR = 1) NSCLC tumors (32).

We explored the mechanism of synergy for dual EGFR and IGF-IR blockade in epithelial tumor cells. The ability of EGFR and IGF-IR to cooperatively affect cell growth is unique to these specific RTKs, and not other RTKs, in a panel of 42 evaluated, as only the activation states for EGFR and IGF-IR were up-regulated in cells treated with the reciprocal inhibitors of these receptors. The observation that inhibition of IGF-IR or EGFR results in rapid up-regulation of the activity for the reciprocal receptors illustrates the plasticity of tumor cells to evoke resistance to inhibition of a single RTK.

RTKs may rely on overlapping cellular machinery to transduce signals, and we investigated the mechanism responsible for cooperative control of growth and survival. Previous reports have shown that EGFR directs activities within both the MAPK and Akt pathways in epithelial, but not mesenchymal-like, tumor cells. Herein, we describe how Akt activity is cooperatively controlled by both EGFR and IGF-IR. Inhibitors of both receptors could partially block Akt activity transiently, and here, the combination achieved an additive inhibition of Akt activity. However, rapid resistance developed such that inhibition of Akt by the single-agent EGFR or IGF-IR inhibitors could not be fully sustained after prolonged treatment. By 24 hours, EGFR inhibitor treatment had conferred a potentiation of IGF-driven Akt, and the combination of both EGFR and IGF-IR antagonists synergistically inhibited Akt to drive apoptosis.

In addition to receptor reciprocity between EGFR and IGF-IR, we find that disruption of EGFR-driven activity within the MAPK pathway contributes to the potentiation of IGF-driven Akt signaling, and this is likely mediated by augmented coupling of IGF-IR to Akt through the IRS-1 adaptor. The ability of IRS-1 phosphorylation at selected serine sites to down-regulate activity is well described (26–28). Previous reports have shown that rapamycin can promote IGF-driven Akt activity by affecting a negative feedback loop imposed on IGF-IR-IRS-1 signaling. Here, blockade of the mTOR-p70S6K signaling pathway prevents serine phosphorylation of IRS-1, thereby promoting IGF-IR-IRS-1 coupling and enhanced capacity to activate the Akt pathway. In this study, we find that blockade of activity within the MAPK pathway, through either upstream inhibition of EGFR or downstream inhibition of MEK, conferred a decrease in IRS-1 serine phosphorylation, promoting IGF-IR-Akt signaling. The synergism that occurs upon dual EGFR and IGF-IR antagonism occurred only in epithelial tumor cells, where EGFR directs the MAPK pathway. A specific inhibitor of MEK evoked a similar decrease in pS-IRS-1 that was associated with an increase in IGF-driven pAkt and accompanied synergistic growth inhibition upon IGF-IR blockade. The ability of the MAPK pathway to affect the serine phosphorylation of IRS-1 could be mediated either directly through Erk or indirectly through the ability of Erk to transactivate p70S6K, as illustrated in Fig. 6*D*. Previous reports have shown that Erk can phosphorylate IRS-1 *in vitro*, and the role of MAPK in feedback inhibition of insulin signaling and insulin resistance has been previously noted (30). In this manner, the mechanism underlying cooperative growth inhibition achieved by combining an IGF-IR antagonist with an EGFR antagonist or MEK antagonist parallels that for an IGF-IR antagonist and rapamycin, where all circumvent negative regulatory feedback loops that converge on IRS-1.

Disclosure of Potential Conflicts of Interest

No potential conflicts of interest were disclosed.

Acknowledgments

References

1. Holbro T, Hynes NE. ErbB receptors: directing key signaling networks throughout life. Annu Rev Pharmacol Toxicol 2004;44:195–217.
2. Roskoski R, Jr. The ErbB/HER receptor protein-tyrosine kinases and cancer. Biochem Biophys Res Commun 2004;319:1–11.
3. Levitzki A. EGF receptor as a therapeutic target. Lung Cancer 2003;41 Suppl 1:S9–14.
4. Kurmasheva RT, Houghton PJ. IGF-I mediated survival pathways in normal and malignant cells. Biochim Biophys Acta 2006;1766:1–22.
5. Chakravarti A, Loeffler JS, Dyson NJ. Insulin-like growth factor receptor I mediates resistance to anti-epidermal growth factor receptor therapy in primary human glioblastoma cells through continued activation of phosphoinositide 3-kinase signaling. Cancer Res 2002; 62:200–7.
6. Gooch JL, Van Den Berg CL, Yee D. Insulin-like growth factor (IGF)-I rescues breast cancer cells from chemotherapy-induced cell death-proliferative and anti-apoptotic effects. Breast Cancer Res Treat 1999;56:1–10.
7. Jones HE, Goddard L, Gee JM, et al. Insulin-like growth factor-I receptor signalling and acquired resistance to gefitinib (ZD1839; Iressa) in human breast and prostate cancer cells. Endocr Relat Cancer 2004;11:793–814.
8. Knowlden JM, Hutcheson IR, Barrow D, Gee JM, Nicholson RI. Insulin-like growth factor-I receptor signaling in tamoxifen-resistant breast cancer: a supporting role to the epidermal growth factor receptor. Endocrinology 2005;146:4609–18.
9. Lu Y, Zi X, Zhao Y, Mascarenhas D, Pollak M. Insulin-like growth factor-I receptor signaling and resistance to trastuzumab (Herceptin). J Natl Cancer Inst 2001;93: 1852–7.
10. Nahta R, Yuan LX, Zhang B, Kobayashi R, Esteva FJ. Insulin-like growth factor-I receptor/human epidermal growth factor receptor 2 heterodimerization contributes to trastuzumab resistance of breast cancer cells. Cancer Res 2005;65:11118–28.
11. Turner BC, Haffty BG, Narayanan L, et al. Insulin-like growth factor-I receptor overexpression mediates cellular radioresistance and local breast cancer recurrence after lumpectomy and radiation. Cancer Res 1997;57: 3079–83.
12. Liu B, Fang M, Lu Y, Mendelsohn J, Fan Z. Fibroblast growth factor and insulin-like growth factor differentially modulate the apoptosis and G_1 arrest induced by anti-epidermal growth factor receptor monoclonal antibody. Oncogene 2001;20:1913–22.
13. Morgillo F, Woo JK, Kim ES, Hong WK, Lee HY. Heterodimerization of insulin-like growth factor receptor/epidermal growth factor receptor and induction of survivin expression counteract the antitumor action of erlotinib. Cancer Res 2006;66:10100–11.
14. Hurbin A, Dubrez L, Coll JL, Favrot MC. Inhibition of apoptosis by amphiregulin via an insulin-like growth factor-1 receptor-dependent pathway in non-small cell lung cancer cell lines. Ann N Y Acad Sci 2003;1010:354–7.
15. Ji QS, Mulvihill MJ, Rosenfeld-Franklin M, et al. A novel, potent, and selective insulin-like growth factor-I receptor kinase inhibitor blocks insulin-like growth factor-I receptor signaling in vitro and inhibits insulin-like growth factor-I receptor dependent tumor growth in vivo. Mol Cancer Ther 2007;6:2158–67.
16. Buck E, Eyzaguirre A, Haley JD, Gibson NW, Cagnoni P, Iwata KK. Inactivation of Akt by the epidermal growth factor receptor inhibitor erlotinib is mediated by HER-3 in pancreatic and colorectal tumor cell lines and contributes to erlotinib sensitivity. Mol Cancer Ther 2006;5:2051–9.
17. Buck E, Eyzaguirre A, Barr S, et al. Loss of homotypic cell adhesion by epithelial-mesenchymal transition or mutation limits sensitivity to epidermal growth factor receptor inhibition. Mol Cancer Ther 2007;6:532–41.
18. Thomson S, Buck E, Petti F, et al. Epithelial to mesenchymal transition is a determinant of sensitivity of non-small-cell lung carcinoma cell lines and xenografts to epidermal growth factor receptor inhibition. Cancer Res 2005;65:9455–62.
19. Frederick BA, Helfrich BA, Coldren CD, et al. Epithelial to mesenchymal transition predicts gefitinib resistance in cell lines of head and neck squamous cell carcinoma and non-small cell lung carcinoma. Mol Cancer Ther 2007;6:1683–91.
20. Shrader M, Pino MS, Brown G, et al. Molecular correlates of gefitinib responsiveness in human bladder cancer cells. Mol Cancer Ther 2007;6:277–85.
21. Yauch RL, Januario T, Eberhard DA, et al. Epithelial versus mesenchymal phenotype determines in vitro sensitivity and predicts clinical activity of erlotinib in lung cancer patients. Clin Cancer Res 2005;11:8686–98.
22. Cullen KJ, Allison A, Martire I, Ellis M, Singer C. Insulin-like growth factor expression in breast cancer epithelium and stroma. Breast Cancer Res Treat 1992;22: 21–9.
23. Giani C, Cullen KJ, Campani D, Rasmussen A. IGF-II mRNA and protein are expressed in the stroma of invasive breast cancers: an in situ hybridization and immunohistochemistry study. Breast Cancer Res Treat 1996;41:43–50.
24. Buck E, Eyzaguirre A, Haley J, Gibson N, Cagnoni P, Iwata KI. Inhibition of Akt by the EGFR inhibitor erlotinib is mediated by HER3 in pancreatic and colorectal tumor cell lines and contributes to erlotinib-sensitivity. Mol Cancer Ther 2006;5:2051–9.
25. De Craene B, Gilbert B, Stove C, Bruyneel E, van Roy F, Berx G. The transcription factor snail induces tumor cell invasion through modulation of the epithelial cell differentiation program. Cancer Res 2005;65:6237–44.
26. Laviola L, Natalicchio A, Giorgino F. The IGF-I signaling pathway. Curr Pharmaceutic Des 2007;13: 663–9.
27. Liu YF, Herschkovitz A, Boura-Halfon S, et al. Serine phosphorylation proximal to its phosphotyrosine binding domain inhibits insulin receptor substrate 1 function and promotes insulin resistance. Mol Cell Biol 2004;24:9668–81.
28. Paz K, Hemi R, LeRoith D, et al. A molecular basis for insulin resistance. Elevated serine/threonine phosphorylation of IRS-1 and IRS-2 inhibits their binding to the juxtamembrane region of the insulin receptor and impairs their ability to undergo insulin-induced tyrosine phosphorylation. J Biol Chem 1997;272:29911–8.
29. O'Reilly KE, Rojo F, She QB, et al. mTOR inhibition induces upstream receptor tyrosine kinase signaling and activates Akt. Cancer Res 2006;66:1500–8.
30. De Fea K, Roth RA. Modulation of insulin receptor substrate-1 tyrosine phosphorylation and function by mitogen-activated protein kinase. J Biol Chem 1997;272: 31400–6.
31. Obenauer JC, Cantley LC, Yaffe MB. Scansite 2.0: proteome-wide prediction of cell signaling interactions using short sequence motifs. Nucl Acids Res 2003;31: 3635–41.
32. Merrick D, Dziadziuszko B, Szostakiewicz A, et al. High insulin-like grwoth factor 1 receptor (IGF-1R) expression is associated with poor survival in surgically treated non-small cell lung cancer (NSCLC) patients. J Clin Oncol 2007;abstract 7550(June 20 supplement).
33. Hidalgo M, Siu LL, Nemunaitis J, et al. Phase I and pharmacologic study of OSI-774, an epidermal growth factor receptor tyrosine kinase inhibitor, in patients with advanced solid malignancies. J Clin Oncol 2001;19: 3267–79.
34. Petty WJ, Dragnev KH, Memoli VA, et al. Epidermal growth factor receptor tyrosine kinase inhibition represses cyclin D1 in aerodigestive tract cancers. Clin Cancer Res 2004;10:7547–54.
35. Tan AR, Yang X, Hewitt SM, et al. Evaluation of biologic end points and pharmacokinetics in patients with metastatic breast cancer after treatment with erlotinib, an epidermal growth factor receptor tyrosine kinase inhibitor. J Clin Oncol 2004;22:3080–90.

Feedback Mechanisms Promote Cooperativity for Small Molecule Inhibitors of Epidermal and Insulin-Like Growth Factor Receptors

Elizabeth Buck, Alexandra Eyzaguirre, Maryland Rosenfeld-Franklin, et al.

Updated version	Access the most recent version of this article at: http://cancerres.aacrjournals.org/content/68/20/8322
Supplementary Material	Access the most recent supplemental material at: http://cancerres.aacrjournals.org/content/suppl/2008/10/07/68.20.8322.DC1

Cited articles	This article cites 33 articles, 20 of which you can access for free at: http://cancerres.aacrjournals.org/content/68/20/8322.full#ref-list-1
Citing articles	This article has been cited by 29 HighWire-hosted articles. Access the articles at: http://cancerres.aacrjournals.org/content/68/20/8322.full#related-urls

E-mail alerts	Sign up to receive free email-alerts related to this article or journal.
Reprints and Subscriptions	To order reprints of this article or to subscribe to the journal, contact the AACR Publications Department at pubs@aacr.org.
Permissions	To request permission to re-use all or part of this article, use this link http://cancerres.aacrjournals.org/content/68/20/8322. Click on "Request Permissions" which will take you to the Copyright Clearance Center's (CCC) Rightslink site.